An Agonist of Toll-Like Receptor 5 Has Radioprotective Activity in Mouse and Primate Models

Lyudmila G. Burdelya, *et al.*

Science **320**, 226 (2008);
DOI: 10.1126/science.1154986

evaluated species distribution models and Zonation solutions for their taxa. A.R. conducted the geographic information system (GIS) analyses to produce the SAPM priority map (Fig. 2B, black outlines). C.K. and A.C. wrote the initial draft of the manuscript; all authors commented on subsequent drafts.

Supporting Online Material
www.sciencemag.org/cgi/content/full/320/5873/222/DC1
Methods
SOM Text
Figs. S1 to S11
Table S1
References
Extended Acknowledgments
Appendix S1
GIS data of Fig. 2

14 January 2008; accepted 7 March 2008
10.1126/science.1155193

An Agonist of Toll-Like Receptor 5 Has Radioprotective Activity in Mouse and Primate Models

Lyudmila G. Burdelya,[1]* Vadim I. Krivokrysenko,[2]* Thomas C. Tallant,[3] Evguenia Strom,[2] Anatoly S. Gleiberman,[2] Damodar Gupta,[1] Oleg V. Kurnasov,[4] Farrel L. Fort,[2] Andrei L. Osterman,[4] Joseph A. DiDonato,[3] Elena Feinstein,[2]† Andrei V. Gudkov[1,2]†

The toxicity of ionizing radiation is associated with massive apoptosis in radiosensitive organs. Here, we investigate whether a drug that activates a signaling mechanism used by tumor cells to suppress apoptosis can protect healthy cells from the harmful effects of radiation. We studied CBLB502, a polypeptide drug derived from *Salmonella* flagellin that binds to Toll-like receptor 5 (TLR5) and activates nuclear factor–κB signaling. A single injection of CBLB502 before lethal total-body irradiation protected mice from both gastrointestinal and hematopoietic acute radiation syndromes and resulted in improved survival. CBLB502 injected after irradiation also enhanced survival, but at lower radiation doses. It is noteworthy that the drug did not decrease tumor radiosensitivity in mouse models. CBLB502 also showed radioprotective activity in lethally irradiated rhesus monkeys. Thus, TLR5 agonists could potentially improve the therapeutic index of cancer radiotherapy and serve as biological protectants in radiation emergencies.

The toxicity of high-dose ionizing radiation (IR) is associated with induction of acute radiation syndromes (*1*) involving the hematopoietic system (HP) and gastrointestinal tract (GI). The extreme sensitivity of HP and GI cells to genotoxic stress largely determines the adverse side effects of anticancer radiation therapy and chemotherapy (*2*). Development of radioprotectants for medical and biodefense applications has primarily focused on antioxidants that protect tissues (*3*) and cytokines that stimulate tissue regeneration (*4*).

Here, we have explored whether radioprotection can be achieved through suppression of apoptosis, the major mechanism underlying massive cell loss in radiosensitive tissues (*5*–*7*). Specifically, we have attempted to pharmacologically mimic an antiapoptotic mechanism frequently acquired by tumor cells, i.e., constitutive activation of the nuclear factor–κB (NF-κB) pathway (*8*). NF-κB is a transcription factor that plays a key role in cellular and organismal response to infectious agents as a mediator of innate and adaptive immune reactions. The link between NF-κB and the mammalian response to IR has been established by previous work showing that GI radiosensitivity is enhanced in mice with a genetic defect in NF-κB signaling (*9*). Activation of NF-κB induces multiple factors that contribute to cell protection and promote tissue regeneration, including apoptosis inhibitors, reactive oxygen species scavengers, and cytokines. Finally, NF-κB activation is among the mechanisms by which tumors inhibit function of the p53 tumor suppressor pathway (*10*), one of the major determinants of radiosensitivity (*11*).

In order to activate NF-κB in GI cells without inducing acute inflammatory responses, we studied factors produced by benign microorganisms in the human gut that activate NF-κB by binding to Toll-like receptors (TLRs) expressed by host cells (*12*). Stimulation of TLR signaling by commensal microflora plays a protective role in the GI tract (*13*). In particular, we focused on TLR5, which is expressed on enterocytes, dendritic cells (*14*), and endothelial cells of the small intestine lamina propria (*15*). Endothelial cell apoptosis has been identified as an important contributor to the pathogenesis of GI acute radiation syndrome (*16*). The only known ligand and agonist of TLR5 is the bacterial protein flagellin (*17*).

To investigate whether flagellin has in vivo radioprotective activity, we injected flagellin purified from *Salmonella enterica* serovar Dublin (*18*) into NIH-Swiss mice 30 min before total-body γ irradiation (TBI). Treatment with 0.2 mg/kg of body weight of flagellin protected mice from lethal doses of 10 and 13 Gy that induce mortality from HP and GI acute radiation syndromes, respectively (Fig. 1A). Flagellin did not rescue mice from 17 Gy TBI but prolonged their median survival from 7 to 12 days. The dose-modifying factor (DMF, the fold change in irradiation dose lethal for 50% of animals) of CBLB502 in NIH-Swiss mice was 1.6, exceeding that of other radioprotective compounds, such as cytokines or amifostine, used at nontoxic doses (*3*).

To reduce the immunogenicity and toxicity of flagellin, we took advantage of studies that mapped the TLR5-activating domains of flagellin to its evolutionarily conserved N and C termini (Fig. 1B) (*19*). We tested a series of engineered flagellin derivatives for NF-κB activation in vitro (Fig. 1B and fig. S1). The most potent NF-κB activator, designated CBLB502, included the complete N- and C-terminal domains of flagellin separated by a flexible linker (fig. S1). CBLB502 produced in *Escherichia coli* as a recombinant protein retains entirely the NF-κB–inducing activity and exceptional stability of flagellin (*18*), yet is substantially less immunogenic (fig. S2). It is also less toxic than flagellin, with a maximum tolerated dose (MTD) in mice of 25 mg/kg as compared with the 12 mg/kg MTD of flagellin (*20*). Flagellin derivatives that failed to activate NF-κB in vitro did not provide radioprotection in vivo (one example is shown in Fig. 1C), which suggested that activation of TLR5 signaling is necessary for radioprotection.

To test whether CBLB502 retained the radioprotective efficacy of flagellin, we administered a single injection of the compound (0.2 mg/kg) to NIH-Swiss mice 30 min before 13 Gy TBI. The treatment (*18*) rescued more than 87% of mice from radiation-induced death (Fig. 1C). At this radiation dose, the most powerful previously described radioprotectants provided about 54% protection [amifostine (*21*)] or had no protective effect at all [5-androstenediol (5-AED) or Neumune (*22*)] (Fig. 1C). Notably, the moderate protective effect observed with amifostine against 13 Gy TBI required injection of a dose (150 mg/kg) close to its MTD (200 mg/kg in NIH-Swiss mice). CBLB502 showed a significantly stronger protective effect ($P < 0.05$) when it was injected at less than 1% of its MTD.

To address the practicality of CBLB502 as an antiradiation drug, we investigated the time frame for effective administration of the compound at different radiation doses. CBLB502 protected mice against the very high doses of radiation that induce lethal HP or combined HP and GI syndromes (10 Gy and 13 Gy, respectively) only when injected 15 to 60 min before TBI (Fig. 1D). The compound provided no survival benefit if injected before this time interval or after irradiation.

[1]Department of Cell Stress Biology, Roswell Park Cancer Institute, Buffalo, NY 14263, USA. [2]Cleveland BioLabs, Inc. (CBLI), Buffalo, NY 14203, USA. [3]Department of Cell Biology, Lerner Research Institute, Cleveland Clinic, Cleveland, OH 44195, USA. [4]Burnham Institute for Medical Research, La Jolla, CA 92037, USA.

*These authors contributed equally to this work.
†To whom correspondence should be addressed. E-mail: andrei.gudkov@roswellpark.org; efeinstein@cbiolabs.com

However, at a radiation dose of 9 Gy, which killed >90% of control [phosphate-buffered saline (PBS)–injected] mice, CBLB502 provided radioprotective benefits when administered as early as 24 hours before, or up to 1 hour after, irradiation. With injection of CBLB502 1 hour postirradiation, 40% of the CBLB502-treated mice survived as compared with 7% of the control mice (Fig. 1D). Thus, CBLB502 is effective as both protects against and mitigates radiation-induced injury.

We next evaluated the effect of CBLB502 on radiation damage to the GI tract and HP system at the tissue and cellular levels. Treatment of NIH-Swiss mice with 0.2 mg/kg CBLB502 30 min before 15 Gy TBI dramatically reduced the proportion of apoptotic cells in the lamina propria of the small intestine of irradiated mice, including vascular endothelial cells (Fig. 2A and fig. S3A) (*18*). This observation is consistent with the postulated role of endothelial apoptosis in the GI toxicity of radiation (*16*). In addition, we found that the radiation-induced reduction in small intestine crypt size and cell density that was observed in control NIH-Swiss mice was ameliorated by CBLB502 pretreatment (0.2 mg/kg given 1 hour before 15 Gy TBI) (Fig. 2B and fig. S3B). CBLB502 treatment did not preserve the morphology of the small intestine in irradiated MOLF/Ei mice (Fig. 2B), a strain with defective TLR5 response because of a germline mutation (*23*), which suggests that radioprotection by CBLB502 is indeed TLR5-dependent. CBLB502-mediated protection of the GI tract was also illustrated by preservation of crypt stem cells in the small intestine. 5-Bromo-2′-deoxyuridine (BrdU) was used to label proliferating crypt cells in irradiated (13 Gy) NIH-Swiss mice pretreated with PBS or CBLB502 (*18*). PBS-injected mice showed a near-complete loss of crypt stem cells, whereas CBLB502-treated mice

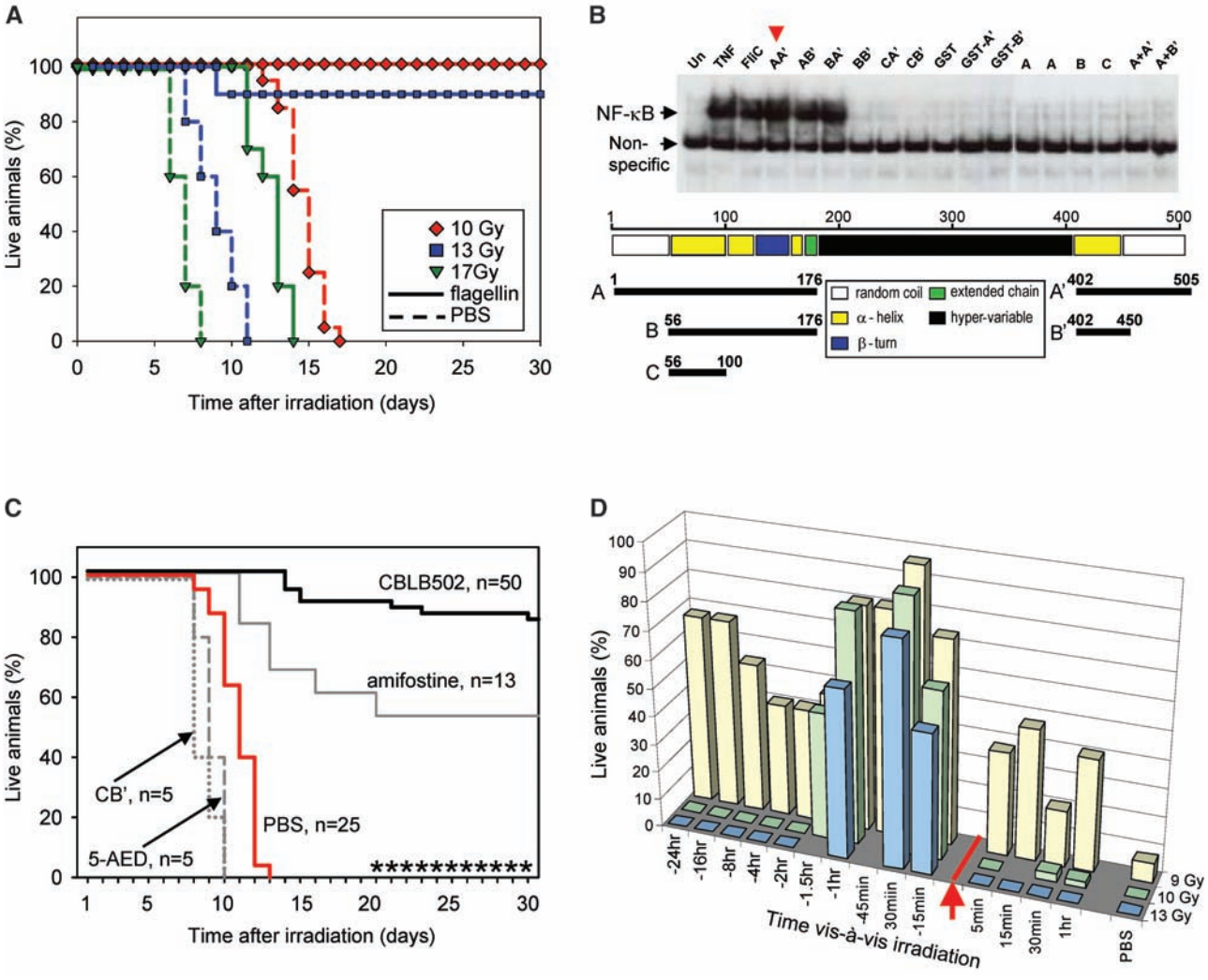

Fig. 1. Flagellin-mediated radioprotection of mice (*18*). (**A**) Groups of 20 NIH-Swiss mice were injected with flagellin or PBS 30 min before TBI. Representative results from one of three independent experiments are shown. The difference in survival between control and experimental groups was statistically significant ($P < 0.05$ by two-tailed Fisher's test) on days 15 to 30, 9 to 30, and 8 to 13 after 10, 13 and 17 Gy TBI, respectively. (**B**) Generation of an optimized flagellin derivative. (Bottom) Schematic of the domain composition of flagellin. Flagellin derivatives were composed from sequences in the conserved N- and C-terminal domains required for TLR5 activation (A, B, and C and A′ and B′, respectively). Amino acid numbering is from flagellin of *Salmonella enterica* serovar Dublin (GenBank accession no. AAA27081). (Top) Assessment of NF-κB activation by flagellin (FliC) derivatives using electrophoretic mobility shift assay. Flagellin itself and variants AA′, AB′, and BA′ induced NF-κB, whereas other combinations of N and C termini (BB′, CA′, and CB′); isolated N termini (A, B, and C); glutathione-*S*-transferase (GST)-fusions of C termini (GST-A′, GST-B′); and mixtures of isolated N and C termini (A+A′, A+B′) were not active. Positive control: TNFα; negative controls: untreated cells (Un) and cells incubated with GST alone (GST). Flagellin variant AA′ (red arrow) was renamed CBLB502. (**C**) NIH-Swiss mice were treated with CBLB502 (0.2 mg/kg), flagellin derivative CB′ (0.2 mg/kg), amifostine (150 mg/kg), 5-AED (30 mg/kg), or PBS before receiving 13 Gy TBI. *$P < 0.03$ by two-tailed Fisher's test for comparison of survival in CBLB502- and amifostine-treated groups. (**D**) ICR mice (15 per group) were injected with CBLB502 at the indicated times relative to 9, 10, or 13 Gy TBI (red arrow). Control mice received PBS 30 min before TBI. The percentage of mice surviving at day 30 post-irradiation is plotted.

retained normal levels of proliferative cells (Fig. 2C and fig. S4).

The antiapoptotic effect of CBLB502 was also evident in the HP system. CBLB502 injection 1 hour before lethal TBI (10 or 13 Gy) of NIH-Swiss mice did not alleviate radiation-induced decreases in bone marrow and peripheral blood cellularity (table S1); however, it did protect HP stem cells and early progenitors as judged by preservation of granulocyte/macrophage colony-forming cells (Fig. 2D) and flow cytometric analysis of stem cell populations in the bone marrow (table S1) (*18*).

To explore potential molecular mechanism(s) that might underlie CBLB502-mediated radioprotection, we assessed the drug's effect on the levels of several known NF-κB–responsive factors. Superoxide dismutase 2 (SOD2) is an NF-κB–induced antioxidant known to have radioprotective properties (*24*). We found that pretreatment of NIH-Swiss mice with CBLB502 (0.2 mg/kg given 30 min before 15 Gy TBI) resulted in enhanced expression of SOD2 in the lamina propria of the small intestine of irradiated mice (Fig. 2E). We also investigated the possible involvement of prostaglandins and cytokines that are regulated by NF-κB and known to act as radioprotectants (*4*, *25*). Inhibition of cyclooxygenase-2 (COX2), a key enzyme in prostaglandin biosynthesis, by a small-molecule inhibitor (NS-398) did not affect CBLB502-mediated radioprotection (fig. S5). However, CBLB502 injection (in the absence of irradiation) led to induction of multiple cytokines in mouse plasma (Fig. 2F), including radioprotective cytokines such as granulocyte colony–stimulating factor (G-CSF) (*26*), interleukin 6 (IL-6) (*27*) and tumor necrosis factor–α (TNFα) (*28*). Consistent with its low toxicity, CBLB502 activated only sub-inflammatory levels of TNFα. These results suggest that CBLB502-mediated radioprotection is likely to involve multiple mechanisms.

CBLB502 was also effective as a radioprotectant in a pilot study of nonhuman primates (*18*). Nineteen rhesus monkeys (*Macaca mulatta*) were subjected to 6.5 Gy (a dose lethal for 70% of

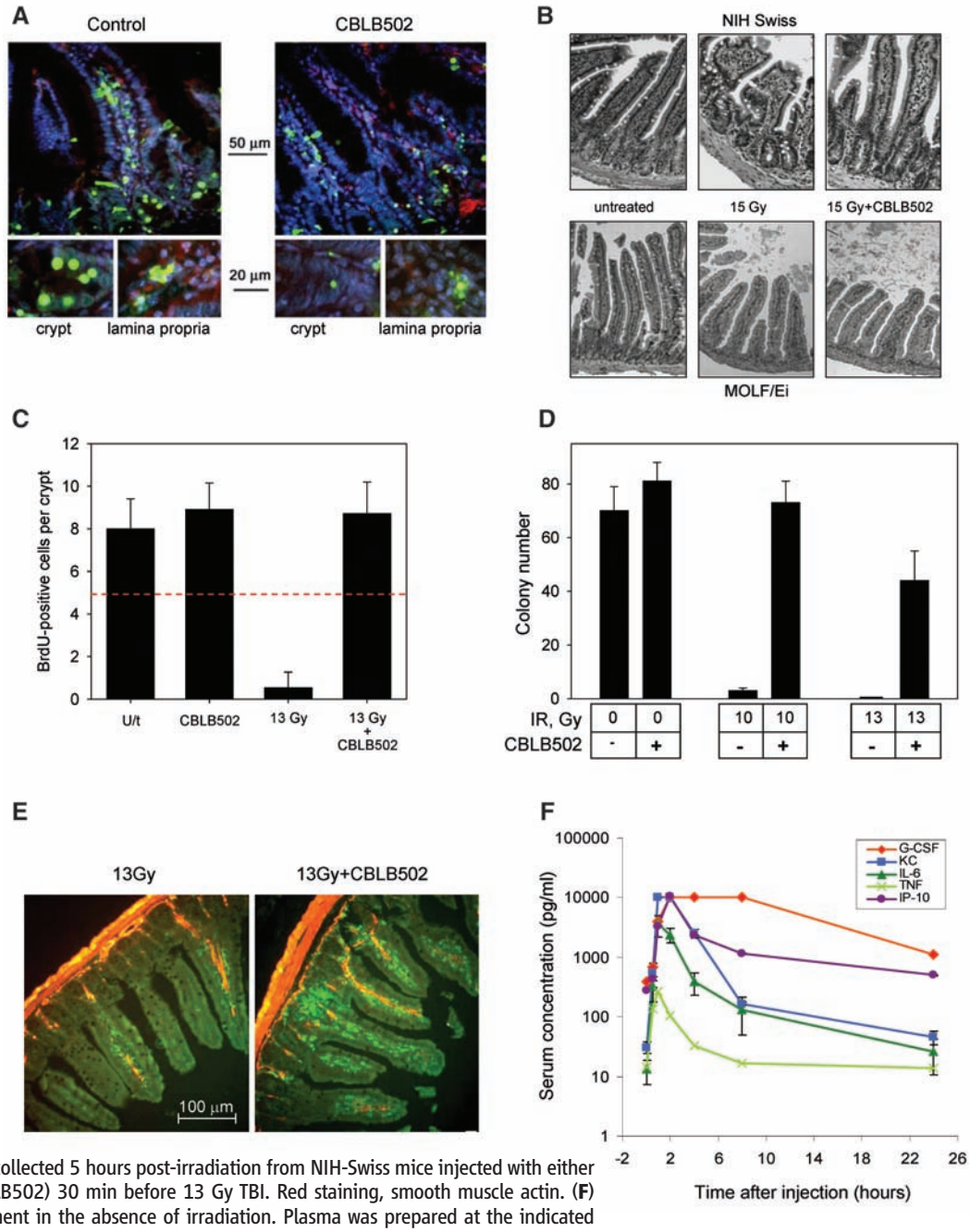

Fig. 2. CBLB502-mediated protection of radiosensitive tissues (*18*). (**A**) Representative terminal deoxynucleotidyl transferase–mediated deoxyuridine triphosphate nick end labeling (TUNEL) staining of apoptotic cells (5 hours postirradiation) in the small intestine of NIH-Swiss mice injected with CBLB502 or PBS 30 min before 15 Gy TBI. Apoptotic endothelial cells displayed yellow fluorescence resulting from overlap of green TUNEL staining and red CD31-specific antibody (endothelial marker) staining. Nuclei were stained with 4′,6′-diamidino-2-phenylindole (DAPI, blue). (**B**) Morphology of the small intestine in NIH-Swiss and MOLF/Ei mice either untreated or 5 days after 15 Gy TBI with or without prior injection of CBLB502. Representative hematoxylin and eosin (H&E) stained sections are shown. (**C**) Immunohistochemical detection of in vivo BrdU incorporation in the crypts of the small intestine. Mice (three per group) were left untreated (U/t), given CBLB502 without TBI (CBLB502), or exposed to 13 Gy TBI 30 min after injection of PBS (13 Gy) or CBLB502 (13Gy + CBLB502). BrdU-positive cells were counted in 12 complete, well-oriented cross sections for each animal. Dashed line: number of BrdU-positive cells considered critical for crypt survival (*36*). $P < 0.05$ for the differences between "13 Gy" and other groups. (**D**) Granulocyte-macrophage colony-forming units were quantified in bone marrow cells obtained from NIH-Swiss mice ($n = 3$) 3 hours after 0, 10, or 13 Gy TBI (with or without CBLB502 injection 30 min before TBI). $P < 0.05$ for the differences between irradiated CBLB502- and vehicle-treated groups. (**E**) Immunohistochemical detection of SOD2 expression (green staining) in sections of small intestine collected 5 hours post-irradiation from NIH-Swiss mice injected with either PBS (13 Gy) or CBLB502 (13Gy + CBLB502) 30 min before 13 Gy TBI. Red staining, smooth muscle actin. (**F**) Cytokine induction by CBLB502 treatment in the absence of irradiation. Plasma was prepared at the indicated times (0.5 to 24 hours) after intramuscular injection of CBLB502 into ICR mice ($n = 3$). KC, keratinocyte-derived chemokine; IP-10, interferon-inducible protein 10.

monkeys, LD_{70}) TBI. Monkeys received a single intramuscular injection of CBLB502 (0.04 mg/kg, $n = 11$) or PBS ($n = 8$) 45 min before TBI. This dose provided a blood concentration of CBLB502 equivalent to 0.2 mg/kg in mice and did not cause any overt signs of toxicity. Injection of CBLB502 before TBI delayed the onset of radiation-induced mortality by 10 days and increased the 40-day survival rate from 25 to 64% (Fig. 3A). Notably, no supportive therapy was provided in this study. Gross and histopathological evaluation of CBLB502-treated monkeys surviving 40 days postirradiation ($n = 7$) revealed only minor damage to major HP and lymphoid organs (bone marrow, spleen, and thymus) (fig. S6). In contrast, the two surviving PBS-treated monkeys displayed moderate-to-high levels of damage in these tissues. Radiation-induced thrombocytopenia, a key predictor of primate death after lethal irradiation (*29*), was less protracted and less severe in CBLB502-treated monkeys than in controls (Fig. 3B).

To assess the potential of CBLB502 as an adjuvant for anticancer radiotherapy, we used two models of experimental radiotherapy in which tumor-bearing mice were subjected to three daily treatments of 4 Gy TBI (a cumulative TBI dose of 12 Gy) (*18*). To evaluate whether CBLB502 affected the radiosensitivity of the tumors, groups of the mice were injected with either PBS or CBLB502 (0.2 mg/kg) 1 hour before each radiation treatment. The two models used were TLR5-positive mouse sarcoma of NIH-Swiss fibroblast origin implanted in NIH-Swiss mice and growing subcutaneously (Fig. 4A) and TLR5-negative B16 melanoma of C57BL/6 origin implanted in C57BL/6 mice (fig. S7). In both models, the antitumor effect of irradiation was accompanied by death of all PBS-treated animals from radiation toxicity by day 18. In contrast, CBLB502 treatment completely prevented radiation-induced mortality [NIH-Swiss mice (Fig. 4A)] or significantly protected against radiation-induced mortality [C57BL6 mice (fig. S7)], but had no radioprotective effect on the tumors. These data illustrate the potential for use of CBLB502 to protect healthy tissues from the adverse side effects of radiotherapy, which are frequently dose-limiting, while not interfering with killing the tumor. These experiments also showed that CBLB502 can protect mice from lethal cumulative damage of fractioned irradiation (three doses of 4 Gy). This is important because radiotherapy of cancer patients is commonly applied as fractioned irradiation. Furthermore, there was no evidence of desensitization with multiple injections of CBLB502. The radioprotective efficacy of CBLB502 injected into ICR mice 30 min before 11 Gy TBI was not affected by previous exposure to the drug with as many as five sequential daily injections (fig. S8). In both mouse tumor models, a slight reduction in tumor growth was observed in CBLB502-treated animals (nonirradiated and irradiated) as compared with corresponding controls. Although these results did not reach statistical significance, they might reflect the known immunostimulatory activity of flagellin (*30*) and other TLR agonists (*31*). The differential radioprotective effect of CBLB502 in tumor versus normal tissues is likely due to the constitutive activation of NF-κB observed in most tumor cells (*32*) and/or inhibition of downstream TLR5 signaling by the activated phosphatidylinositol-3 kinase present in many tumors (*33*).

A theoretical risk of using CBLB502 in cancer treatment is that suppression of apoptosis in-

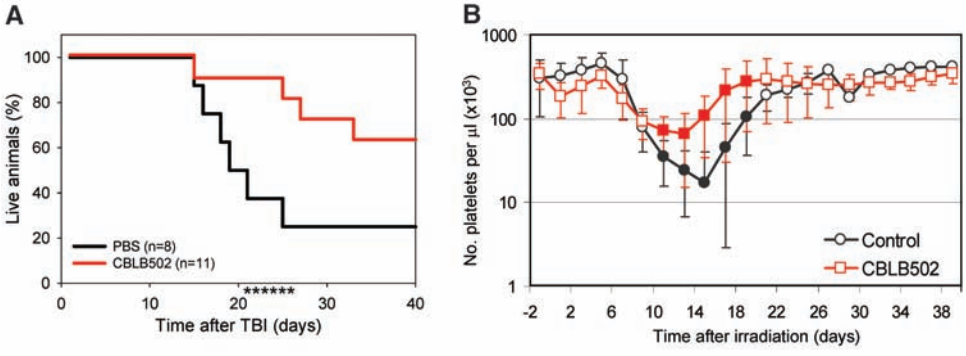

Fig. 3. A single injection of CBLB502 improves survival of lethally irradiated rhesus macaques. (**A**) In a single pilot experiment, rhesus macaques were injected with 0.04 mg/kg CBLB502 ($n = 11$) or PBS ($n = 8$) 45 min before 6.5 Gy TBI ($LD_{70/40}$), a dose lethal for 70% of monkeys within 40 days after irradiation. *$P <$ 0.03 by two-tailed Fisher's test. (**B**) Platelet counts in the peripheral blood of irradiated monkeys. Days with statistically significant ($P <$ 0.05 by two-tailed t test) differences between control and CBLB502 groups are indicated by filled symbols.

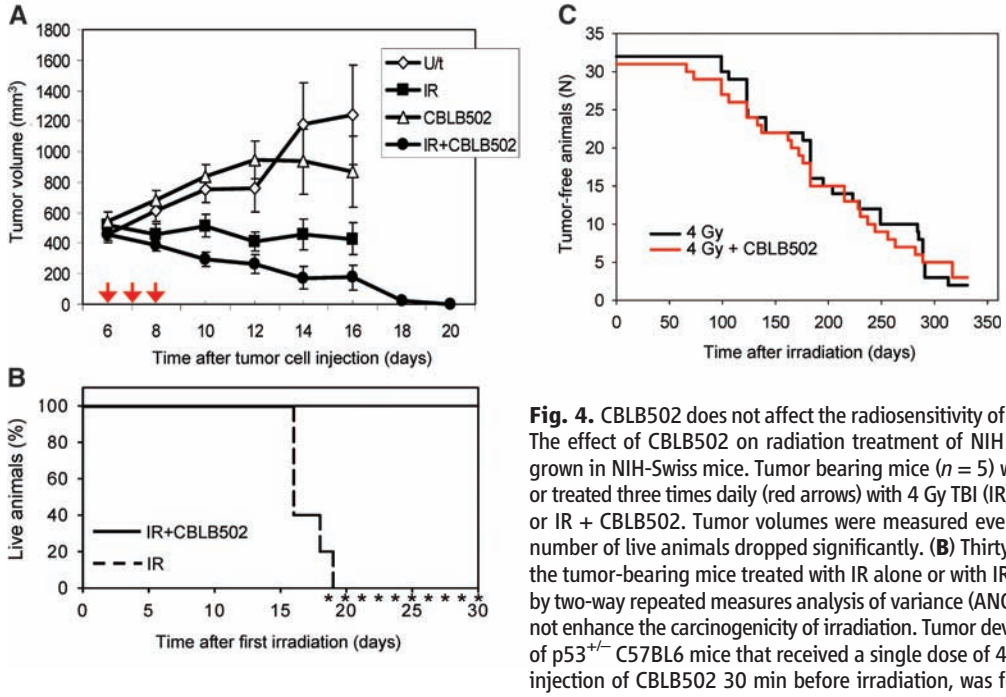

Fig. 4. CBLB502 does not affect the radiosensitivity of mouse tumors (*18*). (**A**) The effect of CBLB502 on radiation treatment of NIH 3T3–derived sarcomas grown in NIH-Swiss mice. Tumor bearing mice ($n = 5$) were left untreated (U/t) or treated three times daily (red arrows) with 4 Gy TBI (IR) alone, CBLB502 alone, or IR + CBLB502. Tumor volumes were measured every second day until the number of live animals dropped significantly. (**B**) Thirty-day survival curves for the tumor-bearing mice treated with IR alone or with IR + CBLB502. *$P < 0.03$ by two-way repeated measures analysis of variance (ANOVA). (**C**) CBLB502 does not enhance the carcinogenicity of irradiation. Tumor development in two groups of $p53^{+/-}$ C57BL6 mice that received a single dose of 4 Gy TBI, with or without injection of CBLB502 30 min before irradiation, was followed for 49 weeks.

duced by systemic genotoxic stress might promote cancer. To address this concern, we tested the effect of CBLB502 on radiation-induced carcinogenicity in cancer-prone $p53^{+/-}$ mice, 100% of which develop tumors (lymphomas and sarcomas) within 1 year after sublethal (4 Gy) TBI (*34*). We found that the timing and frequency of tumor appearance in this model were not affected by a single CBLB502 injection given 30 min before 4 Gy TBI (Fig. 4C). Furthermore, there was no difference in median survival times for TBI-only and CBLB502 + TBI groups: 195 [95% confidence interval (CI): 170 to 220] days versus 195 (95% CI: 144 to 246) days, respectively (log-rank test for equality of distributions: $P = 0.96$). We also evaluated wild-type NIH-Swiss mice that were rescued from lethal irradiation (13 Gy) by CBLB502 treatment 6 months postirradiation. Although the analyzed animals showed signs of radiation-induced tissue damage (cataracts, reduced body weight, and involution of reproductive organs) as compared with age-matched controls that were neither irradiated nor treated, there was no evidence of cancer or massive fibrosis (table S2).

In summary, CBLB502 reduces radiation toxicity without diminishing the therapeutic antitumor effect of radiation and without promoting radiation-induced carcinogenicity. These properties of a TLR5 agonist acting as an NF-κB–inducing agent provide further support for our concept of pharmacological imitation of tumor-specific antiapoptotic mechanisms as an approach to radioprotection. This approach was first validated by our demonstration that a chemical inhibitor of the proapoptotic p53 pathway safeguarded mice from lethal acute radiation syndrome (*11*). However, we subsequently found that wild-type p53 plays an unexpected role as a survival factor in GI cells exposed to high doses of γ-irradiation (*35*), limiting the usefulness of p53 inhibitors to protection against HP, but not GI, acute radiation syndrome. This problem has been resolved by our identification of CBLB502 as a TLR5 agonist that can protect against both major acute radiation syndromes. Our results suggest that TLR5 agonists may be valuable as both adjuvants for cancer radiotherapy and protectants or mitigators for radiation emergencies.

References and Notes

1. J. K. Waselenko *et al.*, *Ann. Intern. Med.* **140**, 1037 (2004).
2. M. J. Dodd, *Managing the Side Effects of Chemotherapy and Radiation* (UCSF Nursing Press, San Francisco, 2001).
3. J. F. Weiss, M. R. Landauer, *Toxicology* **189**, 1 (2003).
4. R. Neta *et al.*, *J. Exp. Med.* **173**, 1177 (1991).
5. A. V. Gudkov, E. A. Komarova, *Nat. Rev. Cancer* **3**, 117 (2003).
6. C. S. Potten, *Cancer Metastasis Rev.* **11**, 179 (1992).
7. R. Kolesnick, Z. Fuks, *Oncogene* **22**, 5897 (2003).
8. M. Karin, *Nature* **441**, 431 (2006).
9. Y. Wang *et al.*, *Cancer Res.* **64**, 6240 (2004).
10. K. V. Gurova *et al.*, *Proc. Natl. Acad. Sci. U.S.A.* **102**, 17448 (2005).
11. P. G. Komarov *et al.*, *Science* **285**, 1733 (1999).
12. C. Pasare, R. Medzhitov, *Adv. Exp. Med. Biol.* **560**, 11 (2005).
13. S. Rakoff-Nahoum, J. Paglino, F. Eslami-Varzaneh, S. Edberg, R. Medzhitov, *Cell* **118**, 229 (2004).
14. S. Uematsu *et al.*, *Nat. Immunol.* **7**, 868 (2006).
15. C. Maaser *et al.*, *J. Immunol.* **172**, 5056 (2004).
16. F. Paris *et al.*, *Science* **293**, 293 (2001).
17. T. Tallant *et al.*, *BMC Microbiol.* **4**, 33 (2004).
18. Materials and methods are available as supporting material on *Science* Online.
19. K. G. Murthy, A. Deb, S. Goonesekera, C. Szabo, A. L. Salzman, *J. Biol. Chem.* **279**, 5667 (2004).
20. T. Eaves-Pyles *et al.*, *J. Immunol.* **166**, 1248 (2001).
21. J. F. Weiss, *Environ. Health Perspect.* **105**, 1473 (1997).
22. M. H. Whitnall *et al.*, *Int. J. Immunopharmacol.* **22**, 1 (2000).
23. G. Sebastiani *et al.*, *Genomics* **64**, 230 (2000).
24. M. W. Epperly *et al.*, *Radiat. Res.* **157**, 568 (2002).
25. K. S. Chun, Y. J. Surh, *Biochem. Pharmacol.* **68**, 1089 (2004).
26. D. C. Dale, *Drugs* **62** (suppl. 1), 1 (2002).
27. K. Atkinson *et al.*, *Cytokines Mol. Ther.* **1**, 47 (1995).
28. L. V. Karkanitsa, M. E. Komarovskaya, S. I. Krivenko, *Stem Cells* **15** (suppl. 2), 95 (1997).
29. D. R. Stickney *et al.*, *Int. Immunopharmacol.* **7**, 500 (2007).
30. A. N. Honko, S. B. Mizel, *Immunol. Res.* **33**, 83 (2005).
31. L. Apetoh *et al.*, *Cancer Genomics Proteomics* **4**, 65 (2007).
32. T. Lu, G. R. Stark, *Cell Cycle* **3**, 1114 (2004).
33. Y. Yu *et al.*, *J. Immunol.* **176**, 6194 (2006).
34. C. J. Kemp, T. Wheldon, A. Balmain, *Nat. Genet.* **8**, 66 (1994).
35. E. A. Komarova *et al.*, *Oncogene* **23**, 3265 (2004).
36. A. Vidrich *et al.*, *Am. J. Pathol.* **166**, 1055 (2005).

37. We thank P. Baker for help with manuscript preparation and editing. Supported by grants CA75179 and AI066497 from NIH and grants from NASA (U.S. National Aeronuautics and Space Administration), the Defense Advanced Research Projects Agency (DARPA) and Cleveland BioLabs, Inc., to A.V.G. and grant CA84406 from NIH to J.A.D. A.V.G., E.F., L.G.B., and J.A.D. have a paid consulting relationship with Cleveland BioLabs, Inc. We dedicate this paper to the memory of our friend and colleague Alexander (Shurik) Neyfakh.

Supporting Online Material

www.sciencemag.org/cgi/content/full/320/5873/226/DC1
Materials and Methods
Figs. S1 to S8
Tables S1 and S2
References

8 January 2008; accepted 12 March 2008
10.1126/science.1154986

Evidence for Editing of Human Papillomavirus DNA by APOBEC3 in Benign and Precancerous Lesions

Jean-Pierre Vartanian, Denise Guétard, Michel Henry, Simon Wain-Hobson*

Cytidine deaminases of the APOBEC3 family all have specificity for single-stranded DNA, which may become exposed during replication or transcription of double-stranded DNA. Three human *APOBEC3A* (*hA3A*), *hA3B*, and *hA3H* genes are expressed in keratinocytes and skin, leading us to determine whether genetic editing of human papillomavirus (HPV) DNA occurred. In a study of HPV1a plantar warts and HPV16 precancerous cervical biopsies, hyperedited HPV1a and HPV16 genomes were found. Strictly analogous results were obtained from transfection experiments with HPV plasmid DNA and the three nuclear localized enzymes: hA3A, hA3C, and hA3H. Thus, stochastic or transient overexpression of *APOBEC3* genes may expose the genome to a broad spectrum of mutations that could influence the development of tumors.

Human APOBEC3 molecules deaminate cytidine residues in single-stranded DNA (ssDNA) and have been demonstrated to have antiviral effects (*1*–*5*). Human immunodeficiency virus–1 (HIV-1) cDNA in particular is vulnerable to the action of the cytoplasmic APOBEC3F and APOBEC3G cytidine deaminases (hA3F and hA3G) (*6*, *7*). Of the seven-gene cluster on chromosome 22, hA3A, hA3C, and hA3H are mainly nuclear, whereas hA3B is both nuclear and cytoplasmic (*8*, *9*). Human *A3A* and *hA3B* are expressed in psoriatic keratinocytes, and *hA3A* is up-regulated in acne lesions and can be induced by phorbol 12-myristate 13-acetate (*10*, *11*). Incidentally, *hA3H* is also expressed in normal skin (*12*, *13*). We hypothesized that the DNA of human papillomaviruses, which replicate in cutaneous and mucosal keratinocytes, might be vulnerable to editing by some of the nuclear A3 deaminases.

In light of the predominant APOBEC3 expression data in cutaneous keratinocytes, total DNA was extracted from six HPV1a-positive plantar warts. For mutational analysis, a region corresponding to the origin of replication/promoter region was selected, because it seemed likely that this region might exist in a single-stranded state more frequently than any other region of the HPV genome. Differential DNA denaturation polymerase chain reaction (3D-PCR) was used to selectively amplify AT-rich edited genomes (*14*, *15*). This technique relies on the fact that AT-rich DNA denatures at a lower temperature than GC-rich

Molecular Retrovirology Unit, Institut Pasteur, 28 Rue de Docteur Roux, 75724 Paris cedex 15, France.

*To whom correspondence should be addressed. E-mail: simon@pasteur.fr